# Novel Function of *Ct*Xyn5A from *Acetivibrio thermocellus*: Dual Arabinoxylanase and Feruloyl Esterase Activity Occur in the Same Active Site

Eva Schmitz[a]*, Savvina Leontakianakou[a]*, Patrick Adlercreutz[a], Eva Nordberg Karlsson[a] and Javier A. Linares-Pastén[a]*

[a] Biotechnology, Department of Chemistry
Lund University
PO Box 124, Lund SE-22100, Sweden
* Corresponding authors: eva.schmitz@biotek.lu.se; savvina.leontakianakou@biotek.lu.se; javier.linares-pasten@biotek.lu.se

**Abstract:** Uncharacterized side activities of enzymes can have significant negative effects on reaction products and yields. Hence, their identification and characterization is crucial for the development of successful reaction systems. Here, we report the presence of feruloyl esterase activity in *Ct*Xyn5A from *Acetivibrio thermocellus* besides its well-known arabinoxylanase activity for the first time. Both reaction types appear to be catalysed in the same active site in two subsequential steps. The ferulic acid substituent is cleaved off first, followed by the hydrolysis of the xylan backbone. The esterase activity on complex carbohydrates was found to be higher than the one of a designated ferulic acid esterase (E-FAERU). Therefore, we conclude that the enzyme exhibits a dual function rather than an esterase side activity.

**Keywords:** enzyme catalysis • multifunctional enzyme • arabino-xylanase • feruloyl esterase • carbohydrates

## Introduction

Enzymes have become widely popular in industry due to their outstanding substrate selectivity and ability to catalyse very specific reactions, thereby minimizing the generation of unwanted by-products[1]. However, they are not perfect in this regard and known to both catalyse reactions other than their main activity as well as accepting different substrates. This feature is suspected to be a result of evolutionary divergence of one multi-function enzyme into a variety of catalytically different enzymes[1a, 2]. Due to the complexity of natural substrates, enzymes with dual functions originating from the presence of two catalytic domains can be found[3].

The additional or side activities of these enzymes are often disregarded in industrial applications. However, they can have significant impacts on the manufacturing process or final product. In the case of dough development, it has been shown that the commonly applied xylanase Pentopan Mono BG impacts the dough's rheological properties via a transglutaminase side activity[4]. Hence, characterizing enzymatic side reactions and multi-functions does not only provide us with a greater understanding of natural biochemical processes, but is also crucial for the development of successful industrial operations and products involving the use of enzymes[5].

Carbohydrate active enzymes are widespread in the food and pharma industries[1b]. Many interesting candidates can be found in the glycoside hydrolase family 5 (GH5), which is characterized by a wide range of members all hydrolysing β-linked oligosaccharides, polysaccharides and glycoconjugates. The recently established subfamily 34 (GH5_34) comprises arabinoxylanases, which are active on the β-1,4 glycosidic linkage between two xylopyranose (Xyl*p*) units of which one is α-1,3-linked to an arabinofuranosyl unit (Ara*f*). This substitution is a requirement that must be present for hydrolysis to occur[6]. Neighboring the -1 subsite (harbouring the catalytic acid base [Glu171] and nucleophile [Glu279]) is a pocket labelled -2* which accommodates and binds to the critical Ara*f* substituent. The three amino acids responsible for this specificity of the active site are Glu68, Tyr92 and Asn139. These are conserved in all members of the family[7].

The first member of this family to be characterized was *Ct*Xyn5A, which is a two domain variant (GH5-CBM6) of the multimodular enzyme from *Acetivibrio thermocellus* ATCC 27405 (previously *Clostridium thermocellum*), a bacterium found in hot springs and self-rotting biomass[6b, 8]. *Ct*Xyn5A is especially accommodating Ara*f* substitutions allowing them in all its subsites ranging from -2 to +2. Therefore, it can act on more highly Ara*f* substituted substrates than classical endo-xylanases found in the glycoside hydrolase families 10 and 11, generating interesting new products[7-8]. Hydrolysis of rye arabinoxylan revealed that all reaction products contained an α-1 Ara*f* substitution linked to the O3 of the Xyl*p* unit at the reducing end. About 30 % of the products contained an additional α-1 Ara*f* substitution. The size of the products ranged between degrees of polymerization (DP) of 2 to 10 with average DPs of 2.8 in the backbone and 4.0 overall[6b, 8a, 9].

In commelinid plants, to which important food crops such as cereals belong, the arabinoxylan often contains a hydroxycinnamic acid substitution at the C5 hydroxy group of its Ara*f* units[10]. Most commonly, comprising 90 % of the cases, this substitution is an esterified ferulic acid (FA)[11]. As self-rotting biomass is the natural habitat of *A. thermocellus*[8b], the *Ct*Xyn5A producer, the enzyme has most likely developed mechanisms to cope with feruloylated arabinoxylans. However, so far there are no reports describing any interactions of *Ct*Xyn5A with feruloylated arabinoxylan[11-12]. Increasing interest in the production of health-promoting arabinoxylo-oligosaccharides (AXOS) as well as feruloylated arabinoxylo-oligosaccharides (FAXOs) demands for a better understanding of the action of GH5_34 members on feruloylated arabinoxylan.

Here we report the interaction of *Ct*Xyn5A, of GH5_34, with FA substitutions on arabinoxylan for the first time. *Ct*Xyn5A was found to exhibit esterase activity, cleaving the FA substitution from the Ara*f* units in complex substrates, hence, making the substrate more accessible for the enzyme's catalytic glycosyl activity. This esterase activity was further characterised on model substrates and explanations of structural mechanisms for the observed behaviours are given.

## Results and Discussion

During our previous study on synergistic enzymatic degradation of pre-treated complex carbohydrates originating from the agricultural side streams oat hull, oat bran and corn bran, the arabinoxylanase *Ct*Xyn5A in combination with a laccase resulted in a similar modification of the lignin fraction as the combination of a ferulic acid esterase (FAE) with the laccase[13]. This observation was only made for these two enzyme combinations, leading us to suspect an esterase side activity of *Ct*Xyn5A. Therefore, the release of ferulic acid (FA) from the two ultrasound assisted alkali pre-treated complex carbohydrates corn bran and oat hull containing a significant amount of FA (see Table 1) was analysed in the present study. *Ct*Xyn5A was found to release more FA from the arabinoxylan backbone than the FAE used (see Figure 1). These data suggest that *Ct*Xyn5A exhibits a rather high esterase activity. Additionally, this esterase activity may increase the arabinoxylanase activity as the removal of the feruloyl-group makes the arabinoxylan backbone more accessible. Due to both of these observations, the enzyme could be classified as multifunctional rather than exhibiting a side activity. The term multifunctionality generally describes an enzyme catalysing more than one biologically relevant reaction[1a].

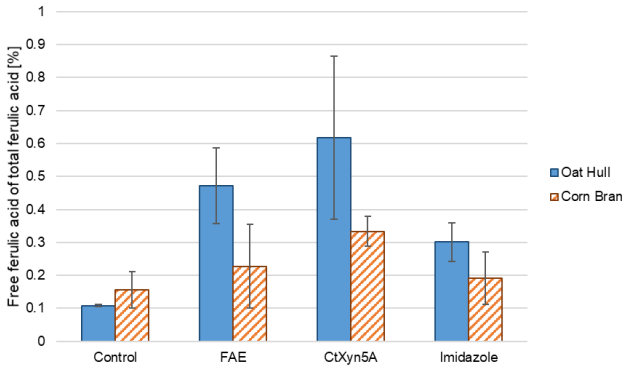


**Figure 1.** Amount of free ferulic acid as percent of the total amount of ferulic acid present in the ultrasound-assisted alkali pre-treated substrates oat hull and corn bran (control) and after reactions with the FAE E-FAERU, *Ct*Xyn5A and imidazole (n = 3).

The commercially available *Ct*Xyn5A formulation from NZYTech contains imidazole, which is used in the elution step in the affinity chromatography, and is necessary for the storage of the enzyme in soluble form. However, imidazole is known to chemically cleave ester bonds[14]. In order to exclude that the presence of imidazole is responsible for the increased ferulic acid release in the reactions with *Ct*Xyn5A, control reactions containing only imidazole in the same concentration as present in the *Ct*Xyn5A formulation were performed. After the imidazole reaction on both oat hull and corn bran the detected amount of free FA was higher than in the control experiment, where no enzyme or imidazole was added, but lower than the amount of free FA present after reaction with imidazole containing *Ct*Xyn5A (see Figure 1). The difference in free FA released can thus be attributed to the action of the *Ct*Xyn5A enzyme itself. Contradicting previous suggestions[11], it therefore seems to be rather unsuitable for the production of feruloylated arabinoxylo-oligosaccharides (FAXOs).

To better characterize the ability of *Ct*Xyn5A to cleave ester bonds, activity assays on the model substrates pNP-butyrate (four carbon chain), pNP-laurate (twelve carbon chain) and pNP-ferulate (most similar to the bond in the complex carbohydrates) were performed, and compared to the activity of the FAE E-FAERU. The results are presented in Figure 2. Both enzymes, as well as imidazole, showed activity on pNP-butyrate (see Figure 2A). The specific activities presented in Table 1 suggest that *Ct*Xyn5A is the more active enzyme on this substrate. However, Figure 2A also shows a significant activity of imidazole on pNP-butyrate. Therefore, this contribution was subtracted from the slope of *Ct*Xyn5A and a specific activity much lower than that of E-FAERU was found (0.036 vs 0.081 µmol/min/mg). In contrast, only E-FAERU was active on both pNP-laurate (Figure 2B) and pNP-ferulate (Figure 2C) with lower, but very similar specific activities of 0.042 and 0.040 µmol/min/mg, respectively. The reaction on pNP-ferulate was furthermore characterized by a rather lengthy lag phase of 40 minutes after which the first pNP cleavages could be detected. These data suggest that the esterase activity of *Ct*Xyn5A is limited to ester bonds linked to rather short chain-substrates with high reactivity, which stands in contrast to the observations on complex carbohydrates. These substrates tend to have a high carbohydrate chain length [15]. Size restrictions would also not explain why the ferulate ester bound to a complex carbohydrate was cleaved rather efficiently, but not when it was linked to pNP. This may instead be caused by interactions with the carbohydrate chain further away from the feruloyl-group.

**Table 1.** Specific activities [µmol/min/mg] of the enzymes ferulic acid esterase (FAE) E-FAERU and *Ct*Xyn5A on the model substrates pNP-butyrate, pNP-laurate and pNP-ferulate at 1 mM concentration.

| Enzyme | pNP-butyrate | pNP-laurate | pNP-ferulate |
|---|---|---|---|
| FAE | 0.081 | 0.042 | 0.040 |
| *Ct*Xyn5A | 0.213 | 0 | 0 |
| *Ct*Xyn5A *Imidazole corrected* | 0.036 | 0 | 0 |

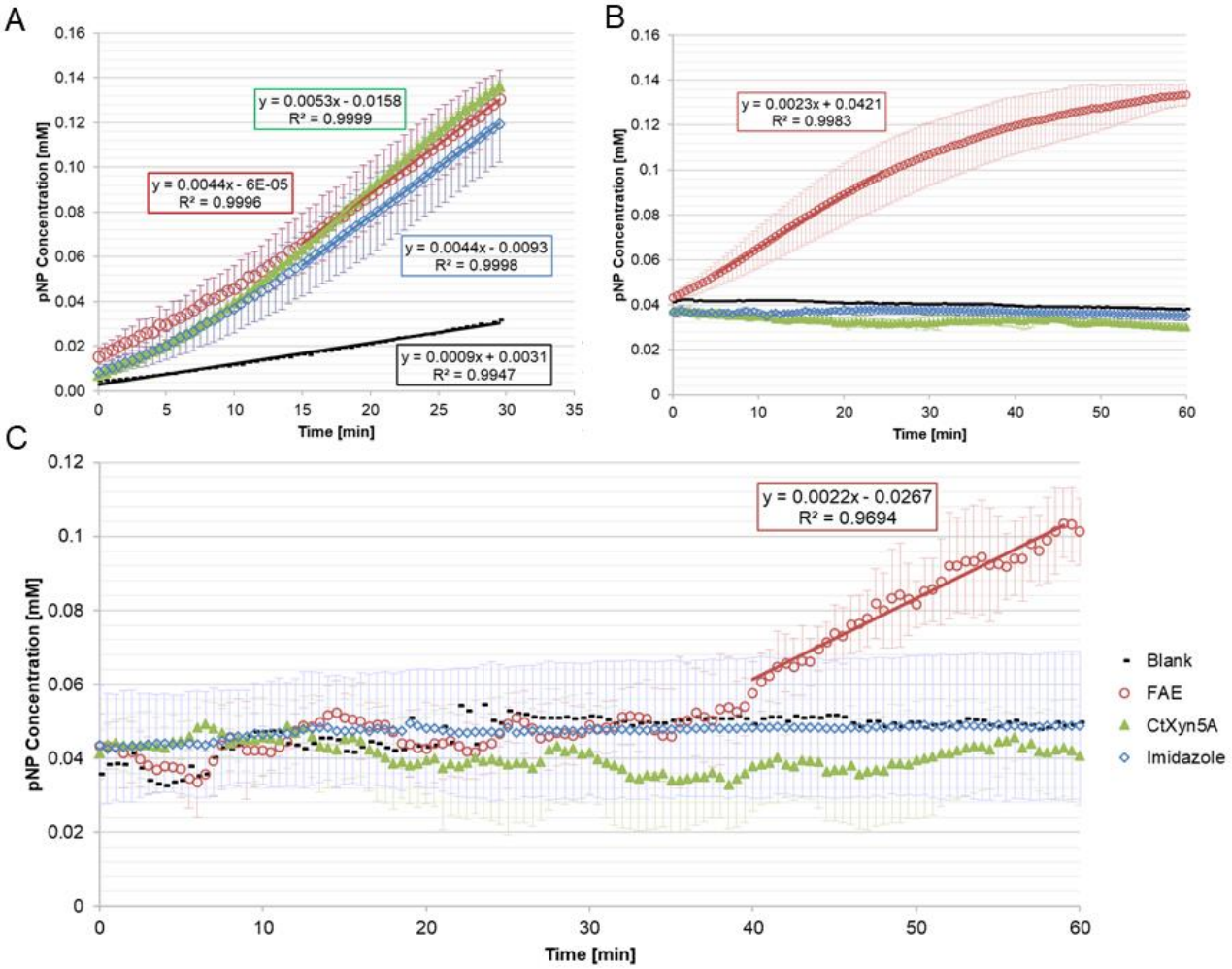


**Figure 2.** Enzyme activity curves describing the amount of pNP released from the substrates pNP-butyrate (A), pNP-laurate (B) and pNP-ferulate (C) by ferulic acid esterase (FAE), *Ct*Xyn5A or imidazole over time in min (n = 3). The equations in the boxes only describe the linear part of each curve. The legend for all graphs can be found in C.

Based on the ambiguous results obtained from the substrate analysis, a point mutation was introduced in which the nucleophile Glu279 in the active site was replaced by a serine. This exchange gives the active site a residue composition more similar to the active sites of typical esterase families. Ferulic acid esterases are characterised by a Ser-His-Asp/Glu catalytic triad in the active site. The serine attacks the carbonyl carbon of the substrate as a nucleophile releasing FA in a multi-step mechanism involving two covalent tetrahedral intermediates[16]. By replacing the stronger nucleophile Glu279 in the active site of *Ct*Xyn5A with the weaker serine, it is hypothesised that the glycosidase activity is eliminated, while the esterase activity is enhanced. Such an effect of a point mutation in the active sites of glucosidases, galactosidases and mannosidases has been reported before[2b]. If such an effect is observed here as well, it can be concluded that both activities originate in the active site and that *Ct*Xyn5A has a dual function, rather than an esterase side activity.

The esterase activity of CtXyn5A-E279S was first characterized using the pNP model substrates (see Figure 3). As observed previously for *Ct*Xyn5A, only activity on the small pNP-butyrate molecule was found. Its imidazole corrected specific activity of 0.032 µmol/min/mg is very low, similar to the one of *Ct*Xyn5A (compare with Table 1), showing that most of the activity can be attributed to the chemical reaction of pNP-butyrate with imidazole.

Unexpectedly, no activity was found on the longer and bulkier substrates pNP-laurate and pNP-ferulate even though its active site resembled the one of the previously screened FAE, which showed activity on all three substrates (compare with Figure 2).

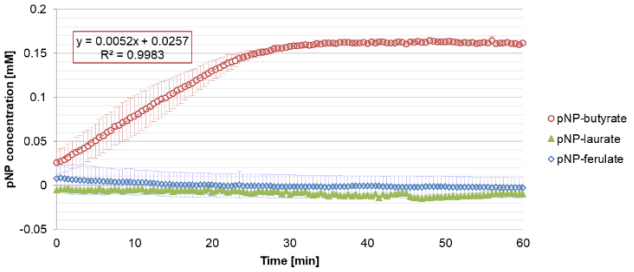


**Figure 3.** Enzyme activity curves describing the amount of pNP released from the substrates pNP-butyrate, pNP-laurate and pNP-ferulate by *Ct*Xyn5A-E279S over time in min (n = 3). The equation in the box only describes the linear part of the pNP-butyrate curve.

After incubation of the CtXyn5A-E279S with the complex substrates oat hull and corn bran, a much higher release of FA was observed compared to both *Ct*Xyn5A as well as E-FAERU (see Figure 4). This increased esterase activity confirms the hypothesis that the catalysis occurs in the active site and that the

enzyme exhibits a dual function, rather than an esterase side activity as discussed previously.

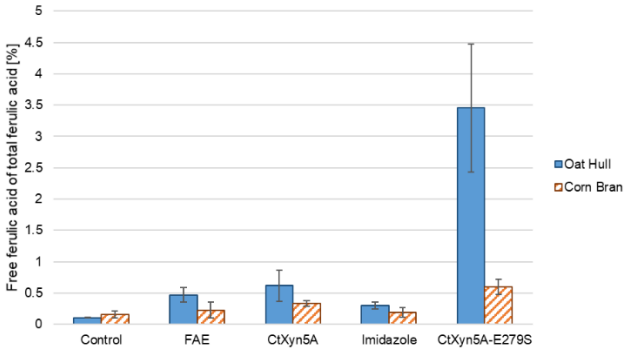


**Figure 4.** Amount of free ferulic acid as percent of the total amount of ferulic acid present in the ultrasound-assisted alkali pre-treated substrates oat hull and corn bran (control) and after reactions with FAE, *Ct*Xyn5A, imidazole and the CtXyn5A-E279S (n = 3).

The Glu to Ser point mutation in the active site of *Ct*Xyn5A was also expected to eliminate the ability of the enzyme to hydrolyse glycosidic bonds. Therefore, the product profile of oat hulls and corn bran was also analysed after reaction with CtXyn5A-E279S. As shown in Figure 5, the chromatograms after reaction with CtXyn5A-E279S are identical to those of the substrates alone, while more hydrolysis products were detected after reaction with CtXyn5A. Therefore, it can be concluded that the introduced mutation eliminated the xylanase activity while it enhanced esterase activity in the same active site.

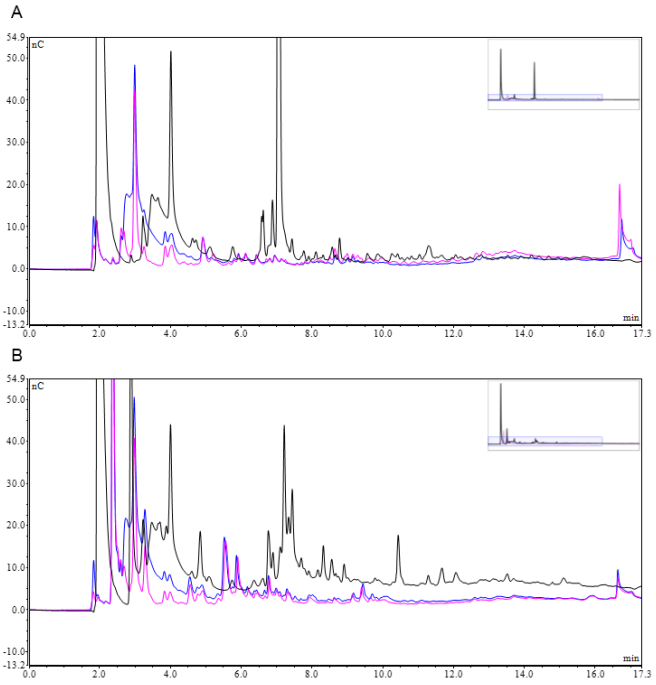


**Figure 5.** HPAEC-PAD chromatograms showing the presence of oligosaccharides in the substrates oat hull (A) and corn bran (B) prior to enzymatic treatment (pink), after treatment with *Ct*Xyn5A (black) and after treatment with CtXyn5A-E279S (blue). The displayed chromatogram is zoomed in to enhance the visibility of the peaks. The full chromatograms are visible in the upper right corners.

Enzymes with both xylanase and feruloyl esterase activity from *A. thermocellus* (previously *Clostridium thermocellum*) have been identified before. However, in those cases, the reactions were catalysed in different domains of a multiprotein complex, the cellulosome[16-17]. To our knowledge for the first time, we have here identified an arabinoxylanase and feruloyl esterase dual function enzyme from *A. thermocellus*, where both reactions are catalysed in the same active site. This finding suggests an interesting and so far unexplored reaction mechanism.

Ligand docking studies revealed two potential binding sites for feruloyl-5-arabino-α-1,3-xyloside in *Ct*Xyn5A: One located in the carbohydrate binding module (CBM6), without any potential catalytic amino acid, and another one in the GH5 catalytic module in the same active site as for the glycoside hydrolysis. Thus, this docking study suggests that the same catalytic site can catalyse both glycoside and ester hydrolysis (Figures 6A and B). The catalytic nucleophile for the glycoside hydrolysis was previously identified as the Glu279[8a], which can also act as a nucleophile for the ester bond hydrolysis of the feruloyl arabinoxylans. As stated above, esterases typically share a conserved catalytic triad: Ser, His, and Asp/Glu, where the Ser is the nucleophile. Based on this fundamental feature, the Glu279 was mutated to Ser (CtXyn5A-E279S), constituting the catalytic triad - Ser279, His253, and Glu171 - comparable to that of the typical esterases. Indeed, this triad shares similar distances between interacting atoms when compared with feruloyl esterases from fungi (*Aspergillus niger*) or bacteria (*A. thermocellus*) (Figures 6C and D), which explains the esterase activity of CtXyn5A-E279S. On the other hand, the Ser is not a suitable nucleophile for catalysing a glycosidic bond hydrolysis, consistent with the functional analysis performed here (Figure 5), and its use as an inactive variant for crystallographic studies[7].

The oxyanion stabilization in typical esterases, including lipases, is through two hydrogen bonds from the amide groups of peptide bonds or via hydrogen (γ-type) of Tyr [18]. In *Ct*Xyn5A or the variant CtXyn5A-E279S, the Tyr255 and Glu171 are in suitable positions to contribute to the oxyanion stabilization (Figure 6F). The distances from the hydroxyl group of Tyr255 and the carboxylic group of Glu171 to the ester carbonyl oxygen are 2.7 and 3.1 Å, respectively, based on the enzyme ligand docking (Figure 6F).

To the best of our knowledge, there are available crystal structures of feruloyl esterases in complex only with ferulic acid (Figures 6E and G), but not with feruloyl-sugars. Different from other feruloyl esterases, *Ct*Xyn5A or CtXyn5A-E279 have activity only with a complex substrate. Therefore, the sugar moiety seems necessary for the enzyme-substrate interaction. The docking with feruloyl-5-arabino-α-1,3-xyloside, shows that the aromatic ring of the feruloyl group fits well in the subsite -2*, and it is stabilized by hydrogen bonds (Glu68 and NH-backbone of Gly136) as well as several hydrophobic interactions (Figure 6F). The ethylene moiety is in subsite -1, with the ester bond close to the catalytic triad, while the sugar moieties bind to the aglycone subsites +1 and +2 (Figures 6F and H). Previous work has suggested that aglycone subsites are less specific than glycone subsites[8a, 9], which is consistent with the possibility of binding arabinose in the +1 subsite. The xylose unit in the +2 subsite has the hydroxyl groups 4 and 1 exposed to the solvent, opening the possibility to extend the xylose backbone in both directions.

With basis on the experimental and computational analysis presented here, we propose that in the presence of a complex substrate, *Ct*Xyn5A first removes the feruloyl group and then

breaks down the xylan backbone. For the esterase activity, residues in the -2*, -1, and aglycone subsites bind to the substrate, while, for the glycoside hydrolase activity, the subsite -2* residues bind to the arabinofuranoside group, and the glycone and aglycone subsite residues create interactions with the xylan backbone as previously described[8a, 9].

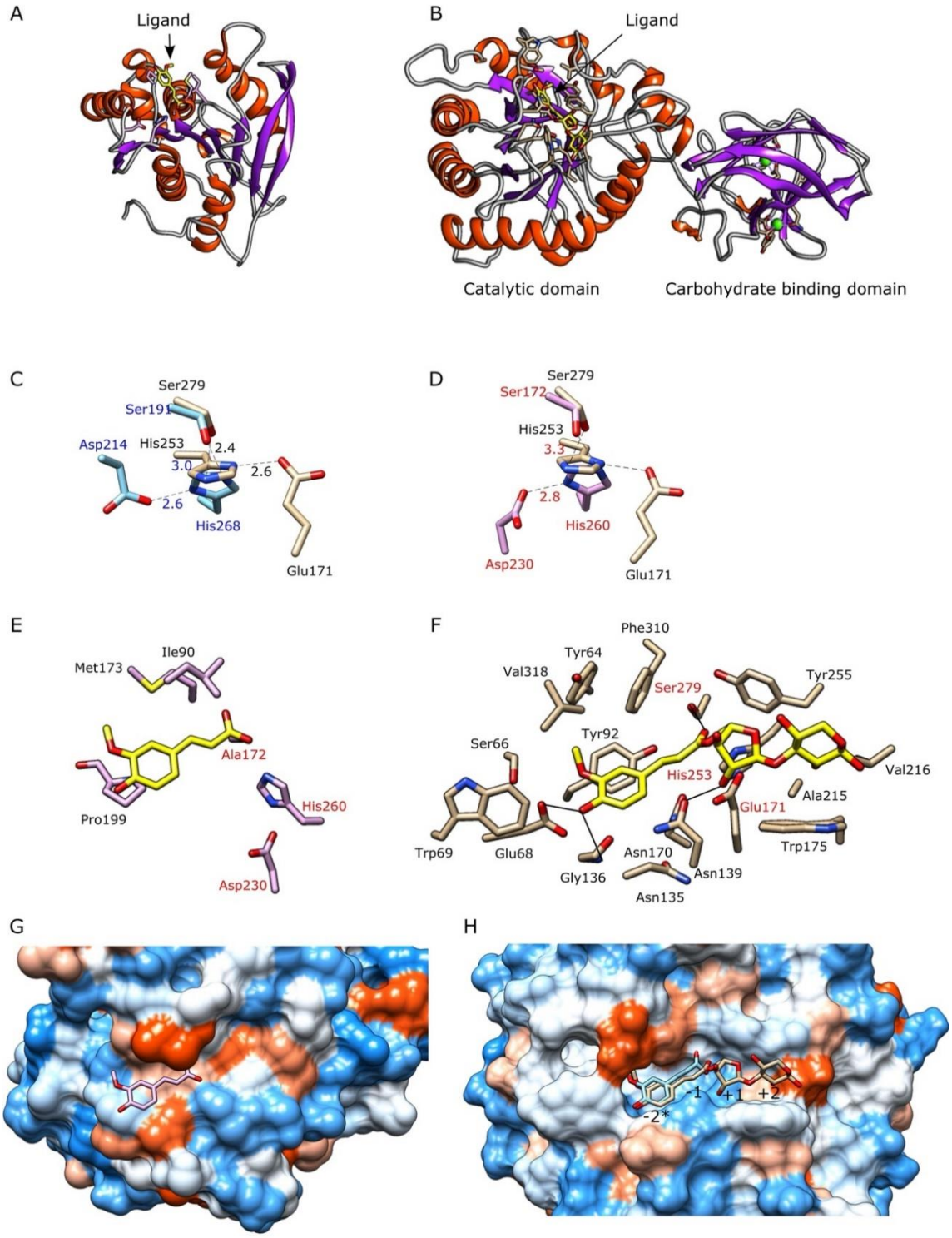


**Figure 6.** Structural analysis of *Ct*Xyn5A-E279S in comparison with feruloyl esterases. (A) Feruloyl domain of the cellulosomal xylanase from *A. thermocellus* (PDB: 1JT2) in complex with ferulic acid. (B) Complex, obtained by docking, CtXyn5A-E279S/feruloyl-5-arabino-α-1,3-xyloside. Overlap of the catalytic triads of the feruloyl esterase from CtXyn5A-E279S (in brown) and *Aspergillus niger* (PDB: 1UWC) (in blue) (C), and *A. thermocellus* (in pink) (D). (E) Amino acids of the feruloyl domain from the ferulolyl esterase (*A. thermocellus*) surrounding the ferulic acid (see also panel A). (F) Amino acids of the catalytic site of CtXyn5A-E279S surrounding the ligand feruloyl-5-arabino-α-1,3-xyloside. Hydrophobicity surface representation (Kyte-Doolitle scale[19]) of the active site of 1JT2 (ferulic acid in pink) (G) and *Ct*Xyn5A-E279S in complex with ferulic acid (in blue) and feruloyl-5-arabino-α-1,3-xyloside (in brown) (H).

## Conclusion

The *Ct*Xyn5A enzyme from *Acetivibrio thermocellus*, previously classified as arabinoxylanase, was found to express a dual function combining arabinoxylanase with feruloyl esterase activity on complex carbohydrate substrates. As its feruloyl esterase activity is higher on carbohydrate polymers, which are expected substrates for the enzyme, compared to a designated ferulic acid esterase, it is concluded that the enzyme exhibits a dual function rather than an esterase side activity. Interestingly, both types of reactions appear to be catalysed in the same active site. Furthermore, by introducing the E279S-mutation a highly promising new ferulic acid esterase, mainly active on carbohydrate polymers, was produced with an increased activity on complex substrates compared to the commercially available E-FAERU.

## Experimental Section

*Substrates, Enzymes and Chemicals*. Two different complex carbohydrate as well as three different model substrates were used in this study. The complex carbohydrates originated from the highly feruloylated agricultural side streams corn bran and oat hull as described in Schmitz *et al*.[13]. Details on their origin and pre-treatment are described in Table 2. The utilized model substrates p-nitrophenyl (pNP) butyrate and pNP-laurate were purchased from Sigma Aldrich, while pNP-ferulate was obtained from Carbosynth. All had a purity of ≥ 98 %. The commercially available ferulic acid esterase (FAE) E-FAERU from Megazyme (Bray, Ireland, 30 U/mg at pH 6.5 and 40 °C) and the truncated arabinoxylanase of glycoside hydrolase family 5 subfamily 34, termed *Ct*Xyn5A (GH5-CBM6) from NZYTech (Lisbon, Portugal, 1 mg/mL, ≥ 90 %) were used in the ester hydrolysis reactions. The imidazole and buffer salts were purchased from Sigma-Aldrich, while the organic solvents were obtained from VWR.

**Table 2.** Description of the origin and prior chemical and enzymatic pre-treatment of the complex carbohydrate substrates used in this study.

| | Corn Bran | Oat Hull |
|---|---|---|
| Variety<br>*Seed origin* | Unknown | Kerstin and Galant<br>*SW-Seed, Sweden* |
| Growth location | USA | Sweden |
| Harvest year | 2019 | 2019 |
| Supplier | Bunge Limited | Lantmännen ek. för. |
| Chemical and enzymatic pre-treatment | Destarching and ultrasound assisted alkali according to [13, 20] | Ultrasound assisted alkali according to [20] |
| Arabinoxylan content [%] | 28.8±1.8 | 20.9±3.3 |
| Ferulic acid content [mg/g] | 227±69 | 90±3 |

*Production and Purification of CtXyn5A-E279S*. The truncated gene encoding the two-domain construct (GH5-CBM6) corresponding to *Ct*Xyn5A from *A. thermocellus*, with the catalytic nucleophile Glu279replaced by Ser (*E279S*) was chemically synthesized (GenScript USA Inc., Piscataway, NJ, USA) with native codons and cloned into the expression vector pET21b (+) with a His-tag introduced to the C-terminus. The resulting plasmid (pET28b:*Ct*Xyn5A-E279S) was transformed into *E. coli* BL21(DE3) competent cells (Sigma) via heat-shock transformation. A 1 % pre-inoculum of the recombinant strain (pre-cultivated in LB medium over night at 37 °C with 100 µg/mL of ampicillin as a selection factor) was added to 300 mL LB medium. The culture was incubated with shaking at 37 °C until an optical density at 600 nm ($OD_{600nm}$) of 0.6-0.8 was obtained. Then it was induced with 1 mM isopropyl β-D-1-thiogalactopyranoside (IPTG) and the incubation was continued at 20 °C overnight. The cells were harvested, lysed by sonication and centrifuged at 26,000 *g* to separate soluble proteins from the cell debris. CtXyn5A-E279S was purified by immobilized metal ion affinity chromatography using an ÄKTA start protein purification system (GE Healthcare Bio-Sciences AB, Uppsala, Sweden) with a HisTrap™ High Performance column (1 mL, Cytiva). The system was equilibrated, and unbound proteins were washed out using a binding buffer consisting of 100 mM Tris-HCl, 500 mM NaCl, pH 7.4. The His-tagged CtXyn5A-E279S was eluted isocratically with a buffer containing 100 mM Tris-HCl, 500 mM NaCl, 365 mM imidazole, pH 7.4. The protein concentration was determined spectrophotometrically by measuring the absorbance at 280 nm and the purity was estimated with sodium dodecyl sulphate-polyacrylamide gel electrophoresis (SDS-PAGE).

*Enzyme and Imidazole Reactions on Complex Carbohydrates*. For the reactions carried out on complex carbohydrates, 50 mg of each of the substrates described in Table 2 was dissolved in 1 mL of 100 mM sodium phosphate buffer (pH 6). To start the reactions, 355 µg of E-FAERU or 10 µg of *Ct*Xyn5A or 10 µg of CtXyn5A-E279S were added. All reactions were performed at 40 °C under constant shaking. After 24 h, they were terminated by boiling at 110 °C for 5 min. To avoid aggregation and precipitation of both *Ct*Xyn5A as well as CtXyn5A-E279S their storage solutions contain up to 2.5 % imidazole (corresponding to 365 mM), which is known to chemically cleave ester bonds[15]. In order to assess its influence on ester bond hydrolysis, a control experiment was carried out in which 2.5 % imidazole in 100 mM sodium phosphate buffer (pH 7.2) was added in the same volume as *Ct*Xyn5A or CtXyn5A-E279S in the enzymatic reactions.

*Free Ferulic Acid Analysis*. The amount of free ferulic acid present in the enzymatic and imidazole reaction mixtures after reaction on the complex carbohydrates was quantified utilizing the HPLC method developed by Sajib and colleagues[21]. In brief, separation of different free phenolic acids was achieved on a Kinetex 2.6 µm Biphenyl 100 Å column (50 mm × 2.1 mm; Phenomenex) under isocratic elution at a flow rate of 0.3 mL/min for 12 min with an Ultimate 3000 Dionex HPLC system. The utilized mobile phase consisted of two mixtures of methanol, acetic acid and Milli-Q water differing in concentration: 87 % of a 10:2:88 mixture and 13 % of a 90:2:8 mixture.

*Esterase Activity Assay*. To further assess the esterase activity and specificity of E-FAERU, *Ct*Xyn5A, CtXyn5A-E279S and imidazole, colorimetric activity assays on pNP-butyrate, pNP-laurate and pNP-ferulate were carried out following the general method first described by Huggins and Lapides[22]. In brief, the substrates were dissolved in solutions of acetonitrile and 2-propanol (1:1) to yield a concentration of 10 mM. In 96-well microtiter plates, 20 µL of these solutions were mixed with 75 µL of Milli-Q water and 100 µL of sodium phosphate buffer (100 mM, pH 7.2). The reactions were started by adding 5 µL of the enzyme or imidazole solutions. The *Ct*Xyn5A, CtXyn5A-E279S and imidazole solutions were used as previously prepared, but the commercial FAE formulation was first diluted 12.5 times to reach a concentration similar to that of *Ct*Xyn5A. The cleavage of pNP from the substrate was monitored via absorbance measurements at 410 nm in a Multiskan Go microplate spectrophotometer (Type 1510, Thermo Scientific) at 37 °C for up to 60 min.

*Oligosaccharide Analysis*. The oligosaccharides present in the pre-treated corn bran and oat hull substrates before and after enzymatic treatment with *Ct*Xyn5A and CtXyn5A-E279S were analysed via HPAEC-PAD (ICS-5000, Dionex, Thermo Scientific). A CarboPac PA200 analytical column (250 mm × 3 mm, 5.5 µm) equipped with a respective guard column (50 mm × 3 mm) was used for separation of the different products. The mobile phase consisted of 100 mM sodium hydroxide and a gradient of sodium acetate of 0-100 mM during the first 10 min after which it was kept constant at 100 mM until the end of the run at 23 min.

*Molecular Modelling*. The molecular structures, available in the Protein Data Bank, *Ct*Xyn5A (PDB: 2Y8K), CtXyn5A-E279S (PDB: 5LA2), and ferulic acid esterase (PDB: 5YAE) from *Streptomyces cinnamoneus,* were used for comparison or docking. All visual analyses and pictures were performed with UCSF Chimera v 1.15[23]. Ferulic acid and feruloyl-5-arabino-α-1,3- xyloside, used as ligands, were modeled in YASARA v 21.12.19[24]. The ligands were energetically minimized with AMBER14[25] force field and subjected to docking with *Ct*Xyn5A, and local docking into the active site of CtXyn5A-E279S using Autodock[26] incorporated in YASARA.

## Acknowledgements

This work is supported by the EU Horizon 2020 project EnXylaScope, Grant number 101000831.

## References

[1] a) A. Peracchi, *Trends Biochem. Sci.* **2018**, *43*, 984-996; b) Q. A. Al-Maqtari, W. AL-Ansi, A. A. Mahdi, *Int. J. Agric. Innov. Res.* **2019**, *8*, 62-82.

[2] a) E. Vlasenko, M. Schulein, J. Cherry, F. Xu, *Bioresour. Technol.* **2010**, *101*, 2405-2411; b) M. D. Toscano, K. J. Woycechowsky, D. Hilvert, *Angew. Chem. Int. Ed.* **2007**, *46*, 3212-3236.

[3] D. O. Krause, S. E. Denman, R. I. Mackie, M. Morrison, A. L. Rae, G. T. Attwood, C. S. McSweeney, *FEMS Microbiol. Rev.* **2003**, *27*, 663-693.

[4] E. Selinheimo, K. Kruus, J. Buchert, A. Hopia, K. Autio, *J. Cereal Sci.* **2006**, *43*, 152-159.

[5] G. Fia, V. Canuti, I. Rosi, *Int. J. Food Sci. Technol.* **2014**, *49*, 1902-1911.

[6] a) H. Aspeborg, P. M. Coutinho, Y. Wang, H. Brumer, B. Henrissat, *BMC Evol. Biol.* **2012**, *12*, 1-16; b) E. Nordberg Karlsson, E. Schmitz, J. A. Linares-Pasten, P. Adlercreutz, *Appl. Microbiol. Biotechnol.* **2018**, *102*, 9081-9088.

[7] A. Labourel, L. I. Crouch, J. L. A. Brás, A. Jackson, A. Rogowski, J. Gray, M. P. Yadav, B. Henrissat, C. M. G. A. Fontes, H. J. Gilbert, S. Najmudin, A. Baslé, F. Cuskin, *J. Biol. Chem.* **2016**, *291*, 22149-22159.

[8] a) M. A. S. Correia, K. Mazumder, J. L. A. Bras, S. J. Firbank, Y. Zhu, R. J. Lewis, W. S. York, C. M. G. A. Fontes, H. J. Gilbert, *J. Biol. Chem.* **2011**, *286*, 22510-22520; b) V. V. Zverlov, K.-P. Fuchs, W. H. Schwarz, *Appl. Environ. Microbiol.* **2002**, *68*, 3176-3179.

[9] P. Falck, J. A. Linares-Pastén, E. Nordberg Karlsson, P. Adlercreutz, *Food Chem.* **2018**, *242*, 579-584.

[10] L. Mkabayi, S. Malgas, B. S. Wilhelmi, B. I. Pletschke, *Agronomy* **2020**, *10*.

[11] S. Lin, J. W. Agger, C. Wilkens, A. S. Meyer, *Annu. Rev. Food Sci. Technol.* **2021**, *12*, 331-354.

[12] P. Biely, S. Singh, V. Puchart, *Biotechnol. Adv.* **2016**, *34*, 1260-1274.

[13] E. Schmitz, S. Leontakianakou, S. Norlander, E. Nordberg Karlsson, P. Adlercreutz, *Bioresour. Technol.* **2022**, *343*, 126114.

[14] a) J. F. Kirsch, W. P. Jencks, *J. Am. Chem. Soc.* **1964**, *86*, 833-837; b) T. Kunitake, F. Shimada, C. Aso, *J. Am. Chem. Soc.* **1969**, *91*.

[15] S. K. Bhatia, S. S. Jagtap, A. A. Bedekar, R. K. Bhatia, A. K. Patel, D. Pant, J. Rajesh Banu, C. V. Rao, Y.-G. Kim, Y.-H. Yang, *Bioresour. Technol.* **2020**, *300*, 122724.

[16] D. W. S. Wong, *Appl. Biochem. Biotechnol.* **2006**, *133*, 87-112.

[17] C. M. G. A. Fontes, G. P. Hazlewood, E. Morag, J. Hall, B. H. Hirst, H. J. Gilbert, *Biochem.* **1995**, *307*, 151-158.

[18] L. Casas-Godoy, S. Duquesne, F. Bordes, G. Sandoval, A. Marty, *Methods Mol. Bio.l* **2012**, *861*, 3-30.

[19] J. Kyte, R. F. Doolittle, *J. Mol. Biol.* **1982**, *157*, 105-132.

[20] E. Schmitz, E. N. Karlsson, P. Adlercreutz, *Waste Biomass Valorization* **2021**, *12*, 5371-5381.

[21] M. Sajib, P. Falck, R. R. R. Sardari, S. Mathew, C. Grey, E. Nordberg Karlsson, P. Adlercreutz, *J. Biotechnol.* **2018**, *268*, 61-70.

[22] C. Huggins, J. Lapides, *J. Biol. Chem.* **1947**, *170*, 467-482.

[23] E. F. Pettersen, T. D. Goddard, C. C. Huang, G. S. Couch, D. M. Greenblatt, E. C. Meng, T. E. Ferrin, *J. Comput. Chem.* **2004**, *25*, 1605-1612.

[24] E. Krieger, G. Vriend, *Bioinformatics* **2014**, *30*, 2981-2982.

[25] D. A. Case, V. Babin, J. Berryman, R. M. Betz, Q. Cai, D. S. Cerutti, P. A. Kollman, **2014**.

[26] O. Trott, A. J. Olson, *J. Comput. Chem.* **2010**, *31*, 455-461.